CHAPTER 6

MOTION CONTROL

In the previous chapter, trajectory planning techniques have been presented which allow generating the reference inputs to the motion control system. Generally speaking, the problem of controlling a manipulator is to determine the time history of the generalized forces (forces or torques) to be developed by the joint actuators so as to guarantee execution of the commanded task while satisfying given transient and steady-state requirements. The task may regard either the execution of specified motions for a manipulator operating in free space, or the execution of specified motions and contact forces for a manipulator whose end effector is constrained by the environment. In view of problem complexity, the two aspects will be treated separately; first, motion control in free space, and then interaction control in constrained space. The problem of *motion control* of a manipulator is the topic of this chapter. A number of *joint space* control techniques are presented. These can be distinguished between *decentralized control* schemes, i.e., when the single manipulator joint is controlled independently of the others, and *centralized control* schemes, i.e., when the dynamic interaction effects between the joints are taken into account. Finally, as a premise to the interaction control problem, the basic features of *operational space* control schemes are illustrated.

6.1 THE CONTROL PROBLEM

Several techniques can be employed for controlling a manipulator. The technique followed, as well as the way it is implemented, may have a significant influence on the manipulator performance and then on the possible range of applications. For instance, the need for trajectory tracking control in the operational space may lead to hardware/software implementations which differ from those allowing point-to-point control where only reaching of the final position is of concern.

On the other hand, the manipulator mechanical design has an influence on the kind of control scheme utilized. For instance, the control problem of a Cartesian manipulator is substantially different from that of an anthropomorphic manipulator.

The driving system of the joints has also an effect on the type of control strategy used. If a manipulator is actuated by electric motors with reduction gears of high ratios,

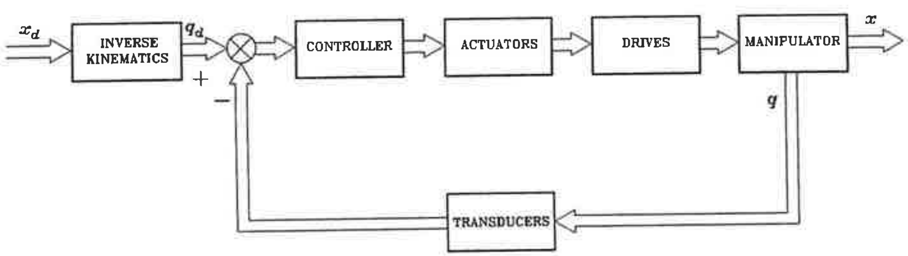

FIGURE 6.1
General scheme of joint space control.

the presence of gears tends to linearize system dynamics and thus to decouple the joints in view of the reduction of nonlinearity effects. The price to pay, however, is the occurrence of joint friction, elasticity and backlash that may limit system performance more than it is due to configuration-dependent inertia, Coriolis forces, and so forth. On the other hand, a robot actuated with direct drives eliminates the drawbacks due to friction, elasticity and backlash but the weight of nonlinearities and couplings between the joints becomes relevant. As a consequence, different control strategies have to be thought of to obtain high performance.

Without any concern to the specific type of mechanical manipulator, it is worth remarking that task specification (end-effector motion and forces) is usually carried out in the operational space, whereas control actions (joint actuator generalized forces) are performed in the joint space. This fact naturally leads to considering two kinds of general control schemes; namely, a *joint space control* scheme (Fig. 6.1) and an *operational space control* scheme (Fig. 6.2). In both schemes, the control structure has closed loops to exploit the good features provided by feedback, i.e., robustness to modeling uncertainties and reduction of disturbance effects. In general terms, the following considerations shall be made.

The *joint space control* problem is actually articulated in two subproblems. First, manipulator inverse kinematics is solved to transform motion requirements from the operational space into the joint space. Then, a joint space control scheme is designed that allows tracking of the reference inputs. However, this solution has the drawback that a joint space control scheme does not influence the operational space variables which are controlled in an open-loop fashion through the manipulator mechanical structure. It is then clear that any uncertainty of the structure (construction tolerance, lack of calibration, gear backlash, elasticity) or any imprecision on the knowledge of the end-effector position relative to an object to manipulate causes a loss of accuracy on the operational space variables.

The *operational space control* problem follows a global approach that requires a greater algorithmic complexity; notice that inverse kinematics is now embedded into the feedback control loop. Its conceptual advantage regards the possibility of acting directly on operational space variables; this is somewhat only a potential advantage, since measurement of operational space variables is often performed not directly, but through the evaluation of direct kinematics functions starting from measured joint space variables.

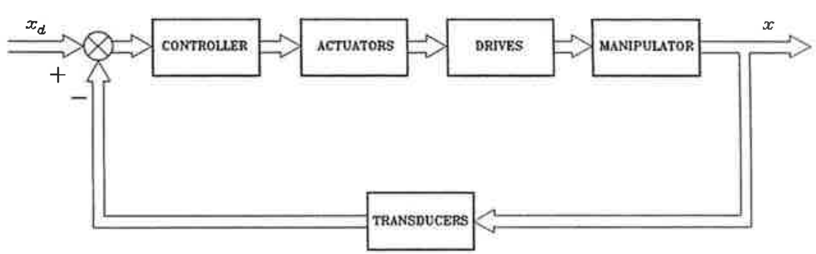

FIGURE 6.2
General scheme of operational space control.

On the above premises, in the following, joint space control schemes for manipulator motion in the free space are presented first. In the sequel, operational space control schemes will be illustrated which are logically at the basis of interaction control in constrained manipulator motion.

6.2 JOINT SPACE CONTROL

In Chapter 4, it was shown that the equations of motion of a manipulator in the absence of external end-effector forces and, for simplicity, of static friction (difficult to model accurately) are described by

$$\boldsymbol{B}(\boldsymbol{q})\ddot{\boldsymbol{q}} + \boldsymbol{C}(\boldsymbol{q},\dot{\boldsymbol{q}})\dot{\boldsymbol{q}} + \boldsymbol{F}_v\dot{\boldsymbol{q}} + \boldsymbol{g}(\boldsymbol{q}) = \boldsymbol{\tau} \tag{6.1}$$

with obvious meaning of the symbols. To control the motion of the manipulator in free space means to determine the n components of generalized forces—torques for revolute joints, forces for prismatic joints—that allow execution of a motion $\boldsymbol{q}(t)$ so that

$$\boldsymbol{q}(t) = \boldsymbol{q}_d(t)$$

as closely as possible, where $\boldsymbol{q}_d(t)$ denotes the vector of desired joint trajectory variables.

The generalized forces are supplied by the actuators through proper transmissions to transform the motion characteristics. Let $\boldsymbol{q}_m$ denote the vector of joint actuator displacements; the transmissions—assumed to be rigid and with no backlash—establish the following relationship

$$\boldsymbol{K}_r\boldsymbol{q} = \boldsymbol{q}_m, \tag{6.2}$$

where $\boldsymbol{K}_r$ is an $(n \times n)$ matrix, usually diagonal in the absence of induced motions, whose elements are much greater than unity.

In view of (6.2), if $\boldsymbol{\tau}_m$ denotes the vector of actuator driving torques, one can write

$$\boldsymbol{\tau}_m = \boldsymbol{K}_r^{-1}\boldsymbol{\tau}. \tag{6.3}$$

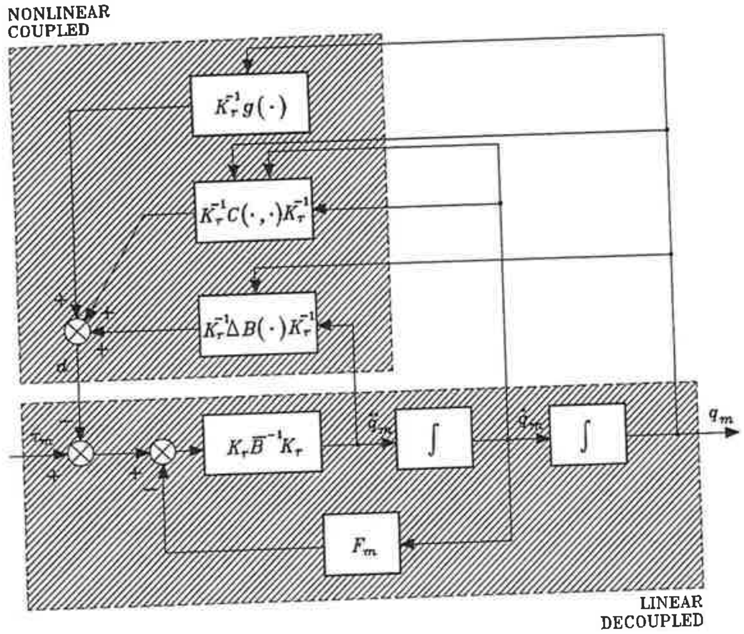

FIGURE 6.3
Block scheme of manipulator with drives.

By observing that the diagonal elements of $B(q)$ are formed by constant terms and configuration-dependent terms (functions of sine and cosine for revolute joints), one can set

$$B(q) = \bar{B} + \Delta B(q) \tag{6.4}$$

where $\bar{B}$ is the *diagonal* matrix whose constant elements represent the resulting average inertia at each joint. Substituting (6.2)–(6.4) into (6.1) yields

$$\tau_m = K_r^{-1}\bar{B}K_r^{-1}\ddot{q}_m + F_m\dot{q}_m + d \tag{6.5}$$

where

$$F_m = K_r^{-1}F_vK_r^{-1} \tag{6.6}$$

represents the matrix of viscous friction coefficients about the motor axes, and

$$d = K_r^{-1}\Delta B(q)K_r^{-1}\ddot{q}_m + K_r^{-1}C(q,\dot{q})K_r^{-1}\dot{q}_m + K_r^{-1}g(q) \tag{6.7}$$

represents the contribution depending on the configuration.

As illustrated by the block scheme of Fig. 6.3, the system of manipulator with drives is actually constituted by two subsystems; one has τ_m as input and q_m as output, the other has q_m, $\dot{q}_m$, and $\ddot{q}_m$ as inputs, and d as output. The former is *linear* and *decoupled*, since each component of τ_m influences only the corresponding component of q_m. The latter is *nonlinear* and *coupled*, since it accounts for all those nonlinear and coupling terms of manipulator joint dynamics.

On the basis of the above scheme, several control algorithms can be derived with reference to the detail of knowledge of the dynamic model. The simplest approach that can be followed, in case of high gear reduction ratios and/or limited performance in terms of required velocities and accelerations, is to consider the component of the nonlinear interacting term d as a *disturbance* for the single joint servo.

The design of the control algorithm leads to a *decentralized* control structure, since each joint is considered independently of the others. The joint controller must guarantee good performance in terms of high disturbance rejection and enhanced trajectory tracking capabilities. The resulting control structure is substantially based on the error between the desired and actual output, while the input control torque at actuator i depends only on the error of output i.

On the other hand, when large operational speeds are required to a direct-drive manipulator ($K_r = I$), the nonlinear coupling terms strongly influence system performance. Therefore, considering the effects of the components of d as a disturbance may generate large tracking errors. In this case, it is advisable to design control algorithms that take advantage of a detailed knowledge of manipulator dynamics so as to compensate for the nonlinear coupling terms of the model. In other words, it is necessary to eliminate the causes rather than to reduce the effects induced by them; that is, to generate compensating torques for the nonlinear terms in (6.7). This leads to *centralized control* algorithms that are based on the (partial or complete) knowledge of the manipulator dynamic model.

Nevertheless, it should be pointed out that these techniques still require the use of error contributions between the desired and the actual trajectory, no matter whether they are implemented in a feedback or in a feedforward fashion. This is a consequence of the fact that the considered dynamic model, even though a quite complex one, is anyhow an idealization of reality which does not include effects, such as joint Coulomb friction, gear backlash, dimension tolerance, and the simplifying assumptions in the model, e.g., link rigidity, and so on.

As pointed out above, the role of the drive system is relevant for the type of control chosen. In the case of decentralized control, the actuator will be described in terms of its own model as a velocity-controlled generator. Instead, in the case of centralized control, the actuator will have to generate torque contributions computed on the basis of a complete or reduced manipulator dynamic model; it will be then considered as a torque-controlled generator which is representative of the actuator/power amplifier system satisfying the above requirement.

6.3 INDEPENDENT JOINT CONTROL

The simplest control strategy that can be thought of is one that regards the manipulator as formed by n independent systems (the n joints) and controls each joint axis as a *single-input/single-output system.* Coupling effects between joints due to varying configurations during motion are treated as disturbance inputs.

In the case of interest, the system to control is joint drive i corresponding to

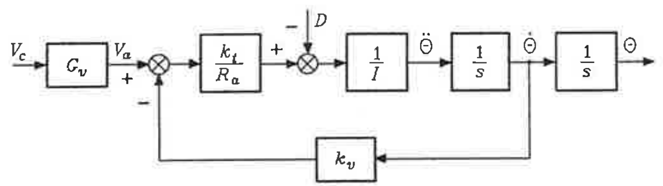

FIGURE 6.4
Block scheme of joint drive system.

the single-input/single-output system of the decoupled and linear part of the scheme in Fig. 6.3. The interaction with the other joints is described by component i of the vector $\boldsymbol{d}$ in (6.7).

Without loss of generality, the actuator is taken as a rotary electric dc motor. Hence, the block scheme of joint i can be represented in the domain of the complex variable s as in Fig. 6.4[1]. In this scheme θ is the angular variable of the motor, I is the average inertia reported to the motor axis ($I_i = \bar{b}_{ii}/k_{ri}^2$), R_a is the armature resistance (auto-inductance has been neglected), and k_t and k_v are respectively the torque and motor constants. Further, G_v denotes the voltage gain of the power amplifier, and then the reference input is not the armature voltage V_a but the input voltage V_c of the amplifier; note that the amplifier bandwidth has been assumed to be much larger than that of the controlled system. In the scheme of Fig. 6.4, it has been assumed also that

$$F_m \ll \frac{k_v k_t}{R_a},$$

i.e., the mechanical viscous friction coefficient has been neglected with respect to the electrical friction coefficient[2].

The input/output transfer function of the motor can be written as

$$M(s) = \frac{k_m}{s(1 + sT_m)}, \tag{6.8}$$

where

$$k_m = \frac{1}{k_v} \qquad T_m = \frac{R_a I}{k_v k_t}$$

are respectively the velocity-to-voltage gain and time constant of the motor.

6.3.1 Feedback Control

To guide selection of the controller structure, start by noticing that an effective rejection of the disturbance d on the output θ is ensured by:

[1] Subscript i has been dropped for notation compactness. Also, Laplace transforms of time-dependent functions are indicated by capital letters without specifying dependence on s.

[2] A complete treatment of actuators is deferred to Chapter 8.

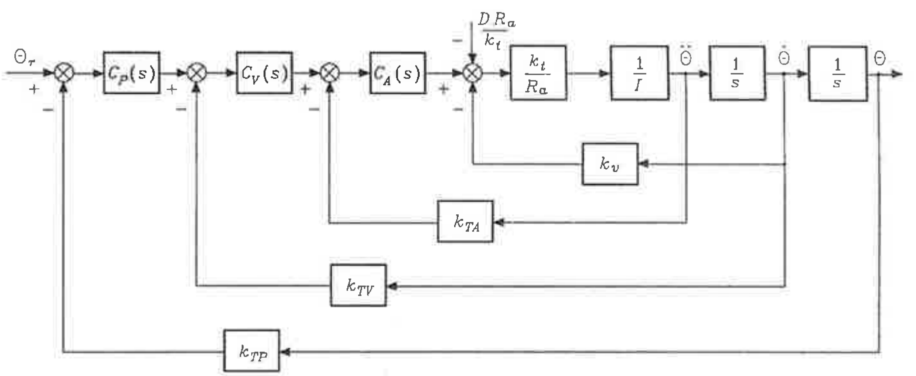

FIGURE 6.5
Block scheme of general independent joint control.

- a large value of the amplifier gain before the point of intervention of the disturbance,
- the presence of an integral action in the controller so as to cancel the effect of the gravitational component on the output at steady state (constant θ).

These requisites clearly suggest the use of a *proportional-integral* (PI) control action in the forward path whose transfer function is

$$C(s) = K_c \frac{1 + sT_c}{s}; \tag{6.9}$$

this yields zero error at steady state for a constant disturbance, and the presence of the real zero at $s = -1/T_c$ offers a stabilizing action. To improve dynamic performance, it is worth choosing the controller as a cascade of elementary actions with local feedback loops closed around the disturbance.

Besides closure of a position feedback loop, the most general solution is obtained by closing inner loops on velocity and acceleration. This leads to the scheme in Fig. 6.5, where $C_P(s)$, $C_V(s)$, and $C_A(s)$ respectively represent *position*, *velocity*, and *acceleration* controllers, where the inmost controller shall be of PI type as in (6.9) so as to obtain zero error at steady state for a constant disturbance. Further, k_{TP}, k_{TV}, and k_{TA} are the respective transducer constants, and the amplifier gain has been embedded in the gain of the inmost controller. In the scheme of Fig. 6.5, notice that the disturbance torque D has been suitably transformed into a disturbance voltage by the factor R_a/k_t.

In the following, a number of possible solutions that can be derived from the general scheme of Fig. 6.5 are presented; at this stage, the issue arising from possible lack of measurement of physical variables is not considered yet. Three case studies are considered which differ in the number of active feedback loops.

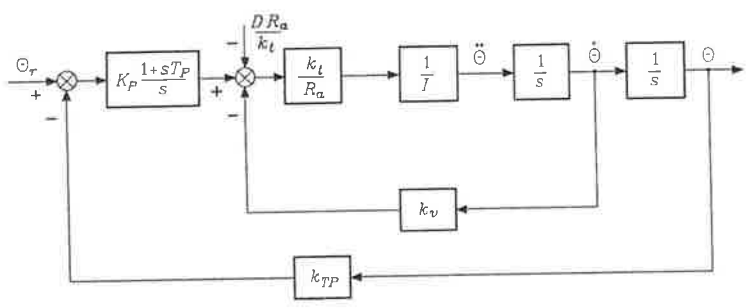

FIGURE 6.6
Block scheme of position feedback control.

Position Feedback. In this case, the control action is characterized by:

$$C_P(s) = K_P \frac{1 + sT_P}{s} \qquad C_V(s) = 1 \qquad C_A(s) = 1$$

$$k_{TV} = k_{TA} = 0.$$

The scheme of Fig. 6.6 shows that the transfer function of the forward path is

$$P(s) = \frac{k_m K_P (1 + sT_P)}{s^2 (1 + sT_m)},$$

while that of the return path is

$$H(s) = k_{TP}.$$

A root locus analysis can be performed as a function of the gain of the position loop $k_m K_P k_{TP} T_P / T_m$. Three situations are illustrated for the poles of the closed-loop system with reference to the relation between T_P and T_m (Fig. 6.7). Stability of the closed-loop feedback system imposes some constraints on the choice of the parameters of the PI controller. If $T_P < T_m$, the system is inherently unstable (Fig. 6.7a). Then, it must be $T_P > T_m$ (Fig. 6.7b). As T_P increases, the absolute value of the real part of the two roots of the locus tending towards the asymptotes increases too, and the system has faster time response. Hence, it is convenient to render $T_P \gg T_m$ (Fig. 6.7c). In any case, the real part of the dominant poles cannot be less than $-1/2T_m$.

The closed-loop input/output transfer function is

$$\frac{\Theta(s)}{\Theta_r(s)} = \frac{\dfrac{1}{k_{TP}}}{1 + \dfrac{s^2 (1 + sT_m)}{k_m K_P k_{TP} (1 + sT_P)}} \qquad (6.10)$$

which can be expressed in the form

$$W(s) = \frac{\dfrac{1}{k_{TP}} (1 + sT_P)}{\left(1 + \dfrac{2\zeta s}{\omega_n} + \dfrac{s^2}{\omega_n^2}\right)(1 + s\tau)},$$

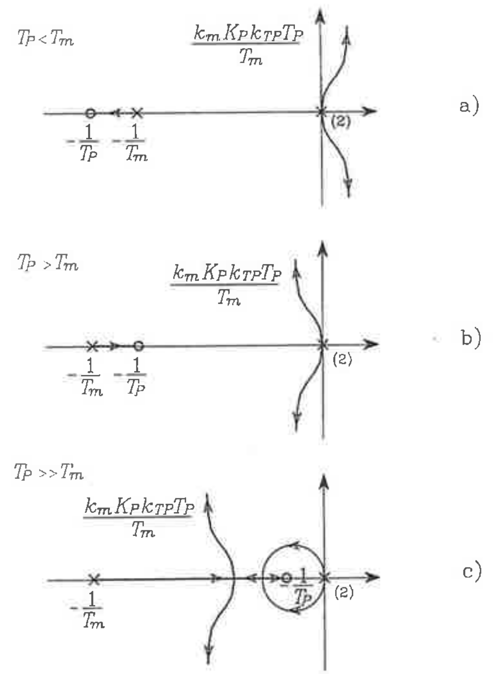

FIGURE 6.7
Root loci for the position feedback control scheme.

where ω_n and ζ are respectively the natural frequency and damping ratio of the pair of complex poles and $-1/\tau$ locates the real pole. These values are assigned to define the joint drive dynamics as a function of the constant T_P; if $T_P > T_m$, then $1/\zeta\omega_n > T_P > \tau$ (Fig. 6.7b); if $T_P \gg T_m$ (Fig. 6.7c), for large values of the loop gain, then $\zeta\omega_n > 1/\tau \approx 1/T_P$ and the zero at $-1/T_P$ in the transfer function $W(s)$ tends to cancel the effect of the real pole.

The closed-loop disturbance/output transfer function is

$$\frac{\Theta(s)}{D(s)} = -\frac{\dfrac{sR_a}{k_t K_P k_{TP} (1 + sT_P)}}{1 + \dfrac{s^2 (1 + sT_m)}{k_m K_P k_{TP} (1 + sT_P)}}, \qquad (6.11)$$

which shows that it is worth increasing K_P to reduce the effect of disturbance on the output during the transient. The function in (6.11) has two complex poles $(-\zeta\omega_n, \pm j\sqrt{1-\zeta^2}\omega_n)$, a real pole $(-1/\tau)$, and a zero at the origin. The zero is due to the PI controller and allows canceling the effects of gravity on the angular position when θ is a constant.

In Eq. (6.11), it can be recognized that the term $K_P k_{TP}$ is the reduction factor imposed by the feedback gain on the amplitude of the output due to disturbance; hence,

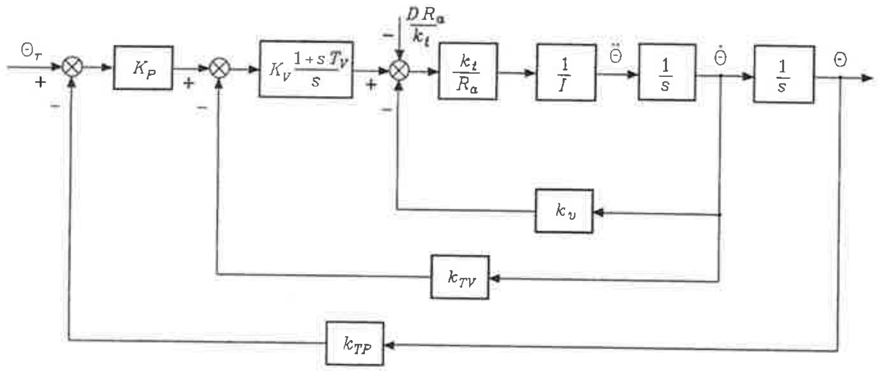

FIGURE 6.8
Block scheme of position and velocity feedback control.

the quantity

$$X_R = K_P k_{TP} \tag{6.12}$$

can be interpreted as the *disturbance rejection factor*, which in turn is determined by the gain K_P. However, it is not advisable to increase K_P too much, because small damping ratios would result leading to unacceptable oscillations of the output. An estimate T_R of the *output recovery time* needed by the control system to recover the effects of the disturbance on the angular position can be evaluated by analyzing the modes of evolution of (6.11). Since $\tau \approx T_P$, such estimate is expressed by

$$T_R = \max\left\{T_P, \frac{1}{\zeta\omega_n}\right\}. \tag{6.13}$$

Position and Velocity Feedback. In this case, the control action is characterized by:

$$C_P(s) = K_P \qquad C_V(s) = K_V\frac{1+sT_V}{s} \qquad C_A(s) = 1$$

$$k_{TA} = 0.$$

To carry out a root locus analysis as a function of the velocity feedback loop gain, it is worth reducing the velocity loop in parallel to the position loop by following the usual rules for moving blocks. From the scheme in Fig. 6.8 the transfer function of the forward path is

$$P(s) = \frac{k_m K_P K_V(1+sT_V)}{s^2(1+sT_m)},$$

while that of the return path is

$$H(s) = k_{TP}\left(1 + s\frac{k_{TV}}{K_P k_{TP}}\right).$$

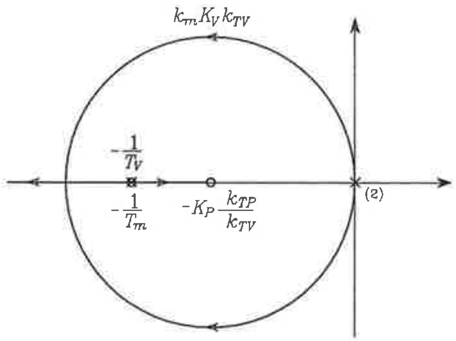

FIGURE 6.9
Root locus for the position and velocity feedback control scheme.

The zero of the controller at $s = -1/T_V$ can be chosen so as to cancel the effects of the real pole of the motor at $s = -1/T_m$. Then, by setting

$$T_V = T_m,$$

the poles of the closed-loop system move on the root locus as a function of the loop gain $k_m K_V k_{TV}$, as shown in Fig. 6.9. By increasing the position feedback gain K_P, it is possible to confine the closed-loop poles into a region of the complex plane with large absolute values of the real part. Then, the actual location can be established by a suitable choice of K_V.

The closed-loop input/output transfer function is

$$\frac{\Theta(s)}{\Theta_r(s)} = \frac{\dfrac{1}{k_{TP}}}{1 + \dfrac{sk_{TV}}{K_P k_{TP}} + \dfrac{s^2}{k_m K_P k_{TP} K_V}}, \tag{6.14}$$

which can be compared with the typical transfer function of a second-order system

$$W(s) = \frac{\dfrac{1}{k_{TP}}}{1 + \dfrac{2\zeta s}{\omega_n} + \dfrac{s^2}{\omega_n^2}}. \tag{6.15}$$

It can be recognized that, with a suitable choice of the gains, it is possible to obtain any value of natural frequency ω_n and damping ratio ζ. Hence, if ω_n and ζ are given as design requirements, the following relations can be found:

$$K_V k_{TV} = \frac{2\zeta\omega_n}{k_m} \tag{6.16}$$

$$K_P k_{TP} K_V = \frac{\omega_n^2}{k_m}. \tag{6.17}$$

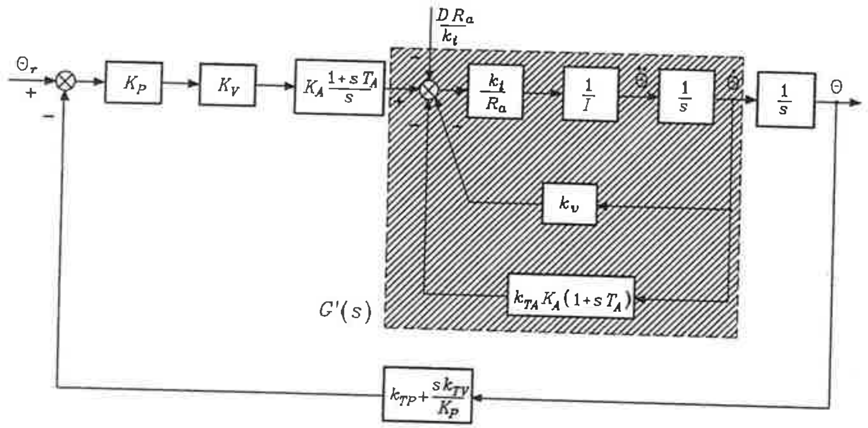

FIGURE 6.10
Block scheme of position, velocity, and acceleration feedback control.

For given transducer constants k_{TP} and k_{TV}, once K_V has been chosen to satisfy (6.16), the value of K_P is obtained from (6.17).

The closed-loop disturbance/output transfer function is

$$\frac{\Theta(s)}{D(s)} = -\frac{\dfrac{sR_a}{k_t K_P k_{TP} K_V (1+sT_m)}}{1 + \dfrac{sk_{TV}}{K_P k_{TP}} + \dfrac{s^2}{k_m K_P k_{TP} K_V}}, \tag{6.18}$$

which shows that the *disturbance rejection factor* is

$$X_R = K_P k_{TP} K_V \tag{6.19}$$

and is fixed, once K_P and K_V have been chosen via (6.16) and (6.17). Concerning disturbance dynamics, the presence of a zero at the origin introduced by the PI, of a real pole at $s = -1/T_m$, and of a pair of complex poles having real part $-\zeta\omega_n$ should be noticed. Hence, in this case, an estimate of the *output recovery time* is given by the time constant

$$T_R = \max\left\{T_m, \frac{1}{\zeta\omega_n}\right\}, \tag{6.20}$$

which reveals an improvement with respect to the previous case in (6.13), since $T_m \ll T_P$ and the real part of the dominant poles is not constrained by the inequality $\zeta\omega_n < 1/2T_m$.

Position, Velocity, and Acceleration Feedback. In this case, the control action is characterized by:

$$C_P(s) = K_P \qquad C_V(s) = K_V \qquad C_A(s) = K_A \frac{1+sT_A}{s}.$$

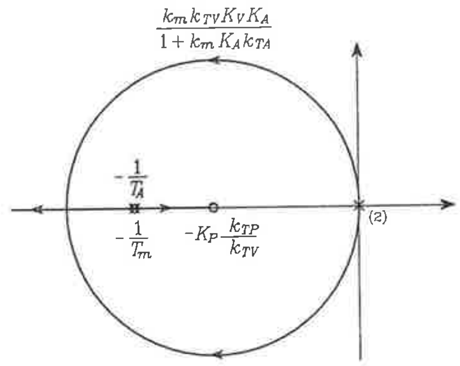

FIGURE 6.11
Root locus for the position, velocity, and acceleration feedback control scheme.

After some manipulation, the block scheme of Fig. 6.5 can be reduced to that of Fig. 6.10 where $G'(s)$ indicates the following transfer function

$$G'(s) = \frac{k_m}{(1 + k_m K_A k_{TA})\left(1 + \dfrac{sT_m\left(1 + k_m K_A k_{TA}\dfrac{T_A}{T_m}\right)}{(1 + k_m K_A k_{TA})}\right)}.$$

The transfer function of the forward path is

$$P(s) = \frac{K_P K_V K_A (1+sT_A)}{s^2} G'(s),$$

while that of the return path is

$$H(s) = k_{TP}\left(1 + \frac{sk_{TV}}{K_P k_{TP}}\right).$$

Also in this case, a suitable pole cancellation is worthy which can be achieved either by setting

$$T_A = T_m,$$

or by making

$$k_m K_A k_{TA} T_A \gg T_m \qquad k_m K_A k_{TA} \gg 1.$$

The two solutions are equivalent as regards dynamic performance of the control system. In both cases, the poles of the closed-loop system are constrained to move on the root locus as a function of the loop gain $k_m K_P K_V K_A/(1+k_m K_A k_{TA})$ (Fig. 6.11). A close analogy with the previous scheme can be recognized, in that the resulting closed-loop system is again of second-order type.